Physical and Mechanical Properties of Poly(methyl methacrylate)-Grafted Natural Rubber Synthesized by Methyl Methacrylate Photopolymerization Initiated by *N*,*N*-Diethyldithiocarbamate Functions Previously Created on Natural Rubber Chains

D. Derouet,[1] Q. N. Tran,[1] J. L. Leblanc[2]

[1]*Laboratoire de Chimie Organique Macromoléculaire, Unité de Chimie Organique Moléculaire et Macromoléculaire (Unité Mixte de Recherche du Centre National de la Recherche Scientifique N°6011), Faculté des Sciences, Université du Maine, Avenue Olivier Messiaen, 72085 Le Mans Cedex 9, France*
[2]*Polymer Rheology and Processing, Université Pierre et Marie Curie, 60 Rue Auber, 94408 Vitry-sur-Seine, France*

ABSTRACT: Well-defined poly(methyl methacrylate) (PMMA)-grafted natural rubbers (NRs) were prepared to study the structure–property relationships. Syntheses were achieved by the photopolymerization of methyl methacrylate initiated by *N*,*N*-diethyldithiocarbamate groups created beforehand in side positions on the NR chains. With this procedure, good control of the graft density and PMMA content could be obtained. Thermal, morphological, and mechanical properties of NR-*g*-PMMA copolymers were studied as a function of the NR/PMMA composition and graft density. NR-*g*-PMMAs containing 15–80% grafted PMMA showed characteristics of heterogeneous materials (characterized by two glass-transition temperatures, those of PMMA and NR, in differential scanning calorimetry). Under these conditions, they developed the morphology of thermoplastic elastomers with PMMA nodules dispersed in the rubber matrix when the PMMA content was near 20%; conversely, they developed the morphology of softened thermoplastics with rubber nodules dispersed in PMMA when the PMMA content was near 80%. Graft copolymers containing about 20% PMMA remained essentially rubbery, but they were already different from pure NR. On the other hand, the thermal stability of NR wash improved after the introduction of PMMA grafts onto NR chains. © 2009 Wiley Periodicals, Inc. J Appl Polym Sci 112: 788–799, 2009

Key words: graft copolymers; mechanical properties; photopolymerization; rheology; rubber

INTRODUCTION

Natural rubber (NR) is an interesting material whose commercial success is due not only to its excellent physical properties (i.e., strength, low heat buildup, excellent flexibility, and impact and tear resistance) but also to the fact that it is a renewable resource. However, NR has some drawbacks, such as low flame resistance, limited resistance to chemicals and solvents, and poor ozone and weathering performance, mainly because of its unsaturated hydrocarbon chain structure. Moreover, its nonpolar character causes limitations in a variety of applications. Therefore, the chemical modification of NR has been widely considered a way of compensating for these disadvantages. Improvements in certain properties, such as gas permeability and oil and flame resistance, have indeed been achieved.[1,2] Among the well-known modified NR products, one can note epoxidized natural rubbers (ENRs),[3–7] maleated NRs,[8–10] and graft copolymers such as poly(methyl methacrylate) (PMMA)-grafted NR[11,12] and polystyrene-grafted NR.[13,14]

Introduced during the late 1950s, thermoplastic elastomers are a relatively new class of materials that combine the physical properties of elastomers, that is, elasticity, and the excellent processing characteristic of thermoplastics.[15–17] From an economic point of view, the consumption of thermoplastic elastomers, since the beginning of the 1980s, has grown by about 6–10% per year. From a structural point of view, they generally consist of two noncompatible phases at the service temperature: a rigid phase that ensures the reinforcement of the material (thermoplastic) and a soft phase that gives its elastic character to the material (elastomer). Each phase has its own glass-transition temperature (T_g), which determines the useful temperature window: T_g is higher than the service temperature for the rigid phase and lower for the soft phase. There are three families of thermoplastic elastomers:
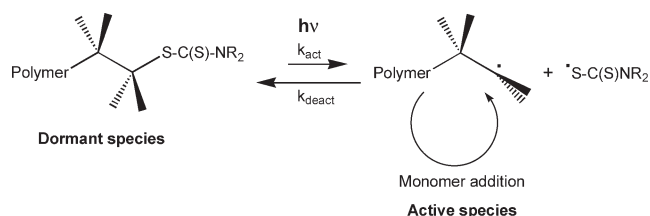
Figure 1 Principle of the photopolymerization of vinyl monomers initiated with iniferters (k_{act} = rate constant of activation; k_{deact} = rate constant of deactivation).

1. Block or graft copolymers made up of macromolecules composed of soft and rigid polymer sequences, particularly triblock copolymers including polystyrene blocks [styrene-butadiene-styrene (SBS), styrene-isoprene-styrene (SIS), and styrene-ethylene-butylene-styrene (SEBS)], which represent roughly 50% of the totality of thermoplastic elastomers. From a structural point of view, the thermoplastic blocks gather to form physical network knots within the polydiene.
2. Thermoplastic elasto-ionomers, whose network knots are thermolabile ionic microdomains formed by associations between ionic groups (carboxylic or sulfonic ones) present on nonpolar polymer chains.
3. Thermoplastic elastomers containing polyolefins [thermoplastic olefin and thermoplastic olefin/dynamically vulcanized (VD)], which are prepared through the physical blending of an elastomer with a plastomer. Sometime, the elastomer phase is slightly crosslinked, and in that case, these materials are called thermoplastic vulcanizates.

Over the last decades, many works have been devoted to the synthesis of thermoplastic-grafted NRs to be used as thermoplastic elastomers. The synthesis of graft copolymers from NR has been carried out in solution,[18,19] on solid rubber,[20] and in latex media.[11–13,21–23] With the objective of improving the grafting yield, we have recently developed a new grafting-from procedure that consists of initiating the radical polymerization of a vinyl monomer from NR chains.[24–26] The principle of the synthesis is based on the pioneering works of Otsu et al. in 1982, who were the first to report the living radical photopolymerization of vinyl monomers initiated from an iniferter (Fig. 1).[27–32]

In this article, we report the mechanical properties (thermal, tensile, and viscoelastic) of copolymers prepared by the grafting of PMMA onto NR according to a method that we recently developed,[24–26] that is, by methyl methacrylate (MMA) photopolymerization initiated by N,N-diethyldithiocarbamate (DEDT) groups introduced beforehand in side positions on the NR chains (Scheme 1). The introduction of DEDT initiating groups along the NR chains was achieved by the addition of sodium N,N-diethyldithiocarbamate trihydrate (DEDT-Na) onto oxirane rings previously created on the chains. The influence of the composition, graft density, and length of grafts on the thermal, mechanical, and rheological properties is hereafter discussed in detail.

EXPERIMENTAL

Materials

Dichloromethane, acetone, methanol, and triethylamine were purified according to standard methods. Tetrahydrofuran was distilled on sodium benzophenone under an argon atmosphere and then stored over 4-Å molecular sieves. DEDT-Na, tetrabutylammonium bromide (TBAB), and toluene were supplied by Acros Organics (a part of Thermo Fisher
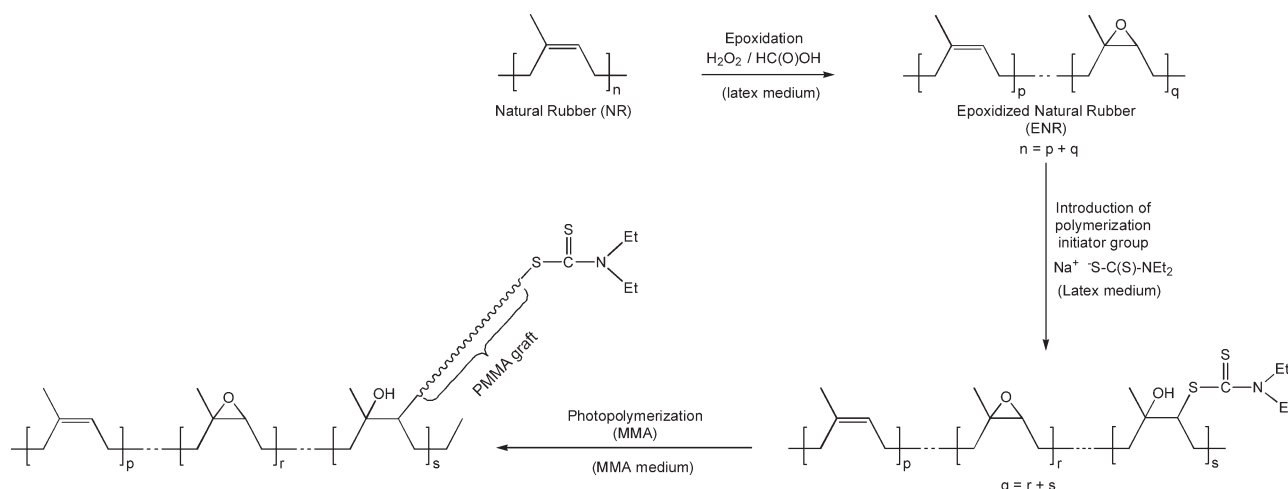
Scheme 1

Scientific, Inc., Cedex, France). The reagents used for the epoxidation of NR latex, that is, 35 wt % hydrogen peroxide and 99 wt % formic acid, were also obtained from Acros Organics. NR latex [42% dry rubber content (drc)] from Thailand and the nonionic surfactant Sinnopal NP 307 (Cognis, Meaux, France) were used without further purification.

Epoxidation of NR latex

ENR latices with various levels of epoxidized units were prepared from NR latex (42% drc) according to a method previously described.[33] Formic acid and hydrogen peroxide were used in equimolar amounts. The amount of hydrogen peroxide was calculated according to the following relation:

$$T = 100 \times [H_2O_2]/[\text{Epoxidized polyisoprene units}]$$

where T is the epoxidation rate required.

Epoxidation rates of synthesized ENRs were determined from their respective ^{1}H-NMR spectra by a comparison of the integration of oxirane ring hydrogens at $\delta = 2.70$ ppm with that of hydrogens of unmodified carbon–carbon double bonds at $\delta = 5.10$ ppm.

Synthesis of *N,N*-diethyldithiocarbamate-functionalized natural rubber (DEDT-NR)

The addition of DEDT-Na onto ENR was carried out in a latex medium according to the method previously described.[24] ENR latex was first diluted to 5% drc, and then Na_2CO_3 was added to adjust the pH to approximately 8 before DEDT-Na and TBAB as a phase-transfer catalyst were introduced. The reaction mixture was stirred at 70°C in a Schlenk flask under a nitrogen atmosphere for 24 h. After the reaction, DEDT-NR was isolated by coagulation in methanol, then washed several times with water, and eventually dried *in vacuo* until a constant weight was obtained. ^{1}H-NMR analysis was used to determine the content in DEDT-NR units.

Synthesis of NR-*g*-PMMAs

NR-*g*-PMMAs were synthesized by the photopolymerization of MMA initiated by DEDT functions on the rubber chains of DEDT-NR according to the grafting-from method that we recently developed.[25,26] Three basic DEDT-NRs with various contents in DEDT-NR units (4.3, 8.1, and 13.6%, respectively) were used to prepare NR-*g*-PMMA copolymers with various structures and compositions. Grafting reactions were carried out at room temperature in an MMA medium. DEDT-NR, previously cut into small pieces, and a quantity of the monomer, selected according to the desired theoretical length of the grafts, were placed in a Schlenk

flask. The mixture was put under a nitrogen atmosphere and then stirred in the dark for 12 h with a mechanical stirring system. Afterwards, the mixture was irradiated for 90 min with a UV lamp (Fisher Bioblock Scientific, Cedex, France) with a wavelength of 365 nm, which was placed 10 cm from the Schlenk flask.

After the grafting, the obtained graft copolymer was coagulated in methanol, entirely isolated, and then washed with water. Finally, it was dried *in vacuo* until a constant weight was obtained.

The PMMA content in the copolymer was determined by weighing. The gross copolymer obtained after drying was weighed and then separated into the graft copolymer and homopolymer by Soxhlet extraction. After drying, the obtained product was weighed and extracted with acetone for 24 h to remove the PMMA homopolymer that possibly formed during the grafting reaction. The residual graft copolymer was recovered and dried *in vacuo* until a constant weight was obtained. The residue (PMMA homopolymer) in the methanol was isolated after methanol evaporation and then dried *in vacuo* for 24 h. The grafting rate (wt %) was calculated as follows:

$$\text{Grafting rate } (\%) = \frac{W_c - W_f}{W_c} \times 100$$

where W_c is the weight of NR-*g*-PMMA obtained after extraction with acetone (i.e., the fraction insoluble in acetone) and W_f is the weight of DEDT-NR before grafting.

Measurements

Liquid ^{1}H-NMR spectra were recorded on a Bruker (Cedex, France) AC 400 Fourier transform spectrometer at 400.13 MHz. Samples were analyzed as solutions in chloroform-D (99.8% purity; Euriso-Top, Gif sur Yvette, France). The chemical shifts are expressed as parts per million on the δ scale with the singlet of tetramethylsilane used as an internal standard.

Thermal characterization of the graft copolymers was carried out with a TA Instrument/Waters (New Castle, DE) Q100 differential scanning calorimeter equipped with a TA Universal Analysis thermal analysis data station and fitted with a mechanical system of cooling by compression [refrigerated cooling system (RCS)] capable of going as low as −90°C. A 3–10-mg sample was placed in the differential scanning calorimetry (DSC) sample pan, and the heating rate was set at 10°C/min. The sample was quenched to −80°C for 1 min, then heated to 160°C to remove the heating history, quenched again to −80°C, and kept at this temperature for 1 min, and the second heating scan from −80 to 160°C was recorded. T_g values were taken at the inflexion point.
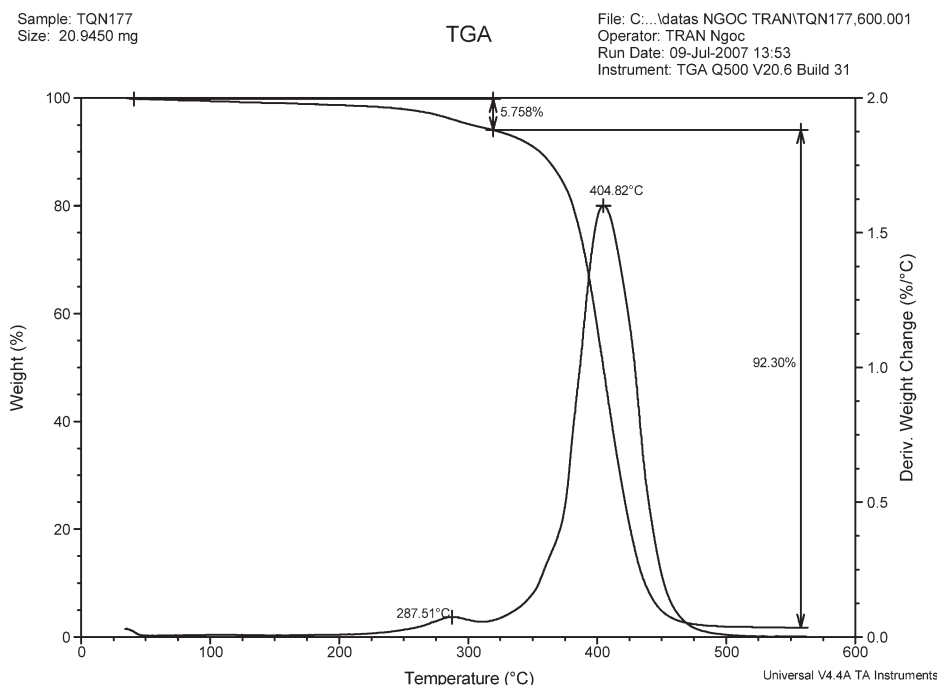
Figure 2 Typical degradation curve of NR2-*g*-PMMA32 obtained under a nitrogen atmosphere.

Thermogravimetric analyses (TGAs) were performed under nitrogen with a TA Instrument/ Waters TGA Q500 instrument equipped with an evolved gas analysis (EGA) oven. A 10–20-mg sample was placed in a platinum pan. Analyses were carried out in a nitrogen atmosphere (gas flow = 100 mL/min) at a heating rate of 20°C/min from 30 to 575°C. At each degradation step, a maximum temperature (T_{max}), corresponding to the maximum degradation rate, was read (Fig. 2).

Tensile and hardness properties of graft copolymers were determined at the Centre de Transfert et Technologies du Mans. NR-*g*-PMMA samples were molded as 2-mm-thick plaques. Molding was carried out at 160°C by the application of a pressure of 90 Bar for 3 min. The plaques were then cooled under 25 tons of pressure for 15 min. Specimens with standard dimensions (Fig. 3) were then cut out with a die.

Tensile characteristics (modulus, elongation at break, and tensile strength) of the PMMA-*g*-NR samples were measured with an MTS Renew tester (Créteil, France). All the tests were made at room temperature with an extensional rate of 20 mm/min.

The elongation at break was calculated with the following equation:

$$\text{Elongation at break } (\%) = \frac{k_r - k_0}{k_0} \times 100$$

where k_0 is the initial length between two marks (10 mm) and k_r is the distance between the marks at break.

The Shore hardness of the specimens was measured at room temperature with a Braive Shore D durometer (Liége, Belgium) according to ASTM D 2240.

The viscoelastic properties of NR-*g*-PMMAs were assessed as follows. Frequency sweep experiments at different temperatures were performed on a series of PMMA-grafted NR samples, with the PMMA content ranging from 20 to 75%, to obtain all data needed to derive master curves of the elastic modulus (G') and viscous modulus (G'') at a reference temperature (T_{ref}). Experiments were performed with a closed-cavity torsional harmonic rheometer [rubber process analyzer (RPA), Alpha Technologies, Dynisco, Akron, OH], a dynamic tester especially designed to handle very stiff materials such as rubbery materials. As illustrated in Figure 4, the test cavity had a biconical geometry and was tightly closed during the measurements by two circular sealing rings.

Samples were received as small chips; they were first compacted into 2-mm-thick sheets through compression molding (200 kPa) at 170°C between polyester foils for 20 min and then cooled to room
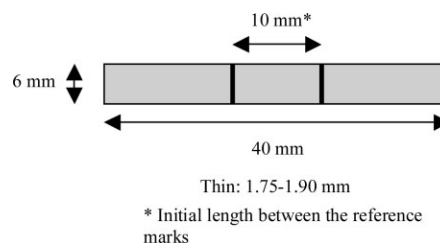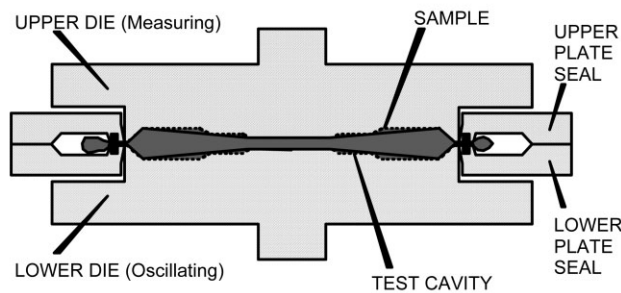

Figure 3 Specimen dimensions.

Closed cavity torsional harmonic rheometer : RPAØ 2000(Alpha Techologies, Dynisco)
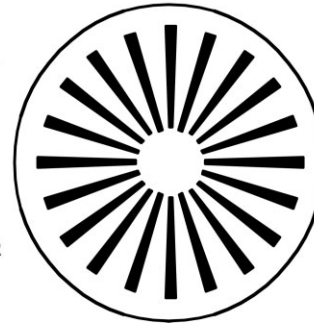

Figure 4 Closed-cavity torsional rheometer: biconical cross-section test cavity and grooved dies.

temperature around a 20-kPa load. Acceptable-quality sheets were obtained, from which 41-mm-diameter disks were die-cut, and their weight was adjusted within the 3.0–3.2-g range to load the rheometer with samples with a volume of around 3.3 cm^3, that is, the test cavity volume plus 10%. To avoid excessive cleaning problems with the test cavity, samples were loaded between polyester circular disks of an appropriate diameter; this is a standard procedure that is known to have marginal effects, if any, on harmonic torque readings with an RPA.

The reference NR sample was tested in the temperature range of 60–160°C, but all PMMA-grafted NR samples were so stiff at temperatures below 120°C that they exceeded the capabilities of the torque transducer. Therefore, all grafted NR samples were tested in the 120–220°C range.

Results in terms of G', G'', and tan δ were collected from RPA test data files and assembled in a worksheet. Typical results for the reference NR samples and a PMMA-grafted NR sample are shown in Figure 5. As expected, in the investigated
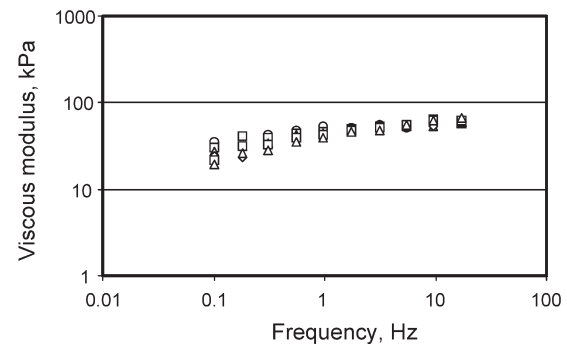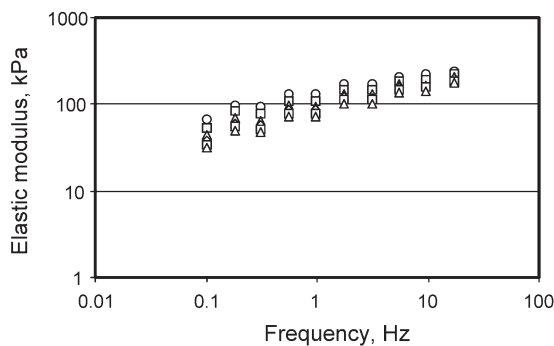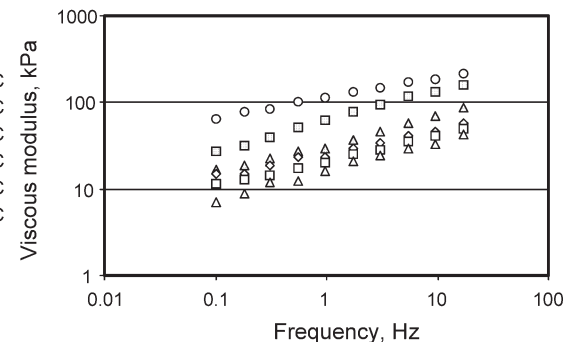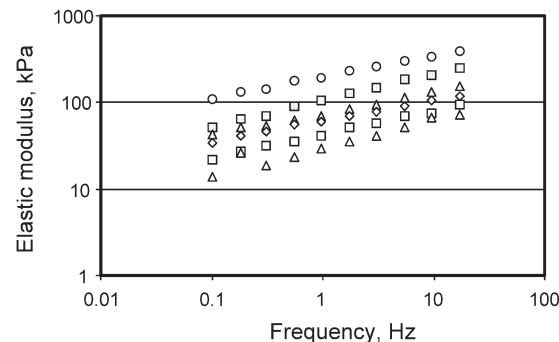

Figure 5 Typical experimental results obtained from frequency sweep experiments with the RPA. The experimental temperature windows were 60–160°C for the NR sample and 120–220°C for the grafted NR.

temperature window, the gum NR was not very temperature-sensitive, essentially because the terminal (flow) zone of the dynamic modulus was investigated. Conversely, the grafted NR exhibited a strong thermal dependence, and experimental curves suggested that T_g was within the experimental temperature window.

Master curves at 120°C were built in agreement with the time–temperature principle first by experimental determination (through a simple graphical procedure) of the approximate values of the shift factor (for G' and G'', respectively) that would resolve the data obtained at different temperatures into a single curve at the selected T_{ref} value. Shift factors were eventually fine-tuned by the fitting of the experimental values to the variation of shift factor $a_T(T_{ref})$ versus the temperature according to a Williams–Landel–Ferry (WLF)-type equation:

$$\log a_T(T_{ref}) = \frac{-C_1(T - T_{ref})}{C_2 + T - T_{ref}}$$

where C_1 and C_2 are fitting parameters. For each sample, the corresponding master curve (either G' or G'') at $T_{ref} = 120$°C and the values of C_1 and C_2 allowed us to recover the modulus functions at any temperature within the experimental range. The reference NR and the grafted NR samples could thus be easily compared at T_{ref}.

The morphology of NR-g-PMMA samples was examined by transmission electron microscopy (TEM; model 2010, JEOL, Peabody, MA) at 300 kV. The samples for analysis were prepared as follows. A drop of 0.3 wt % NR-g-PMMA in chloroform was placed on a carbon-coated Formvar film deposited onto a copper grid. The latter was then thermally treated by DSC under nitrogen with the following program: heating from 20 to 130°C at 20°C/min, a 130°C isotherm for 10 min, cooling from 130 to 80°C at 20°C/min, an 80°C isotherm for 10 min, and finally cooling from 80 to 20°C at 20°C/min. After the thermal treatment, the grid was plunged into a 1 wt % solution of osmium tetroxide (OsO₄) in methanol for 1 h. Ruthenium tetroxide was used to stain the rubber domains.

RESULTS AND DISCUSSION

Three basic DEDT-NRs were synthesized[24] and used as macroinitiators to prepare NR-g-PMMAs with various graft densities and PMMA contents: NR1 (containing 4.3% DEDT-NR units), NR2 (containing 8.1% DEDT-NR units), and NR3 (containing 13.6% DEDT-NR units). PMMA grafting was performed in a Schlenk flask under a nitrogen atmosphere, and UV irradiation was produced with a Fisher Bioblock
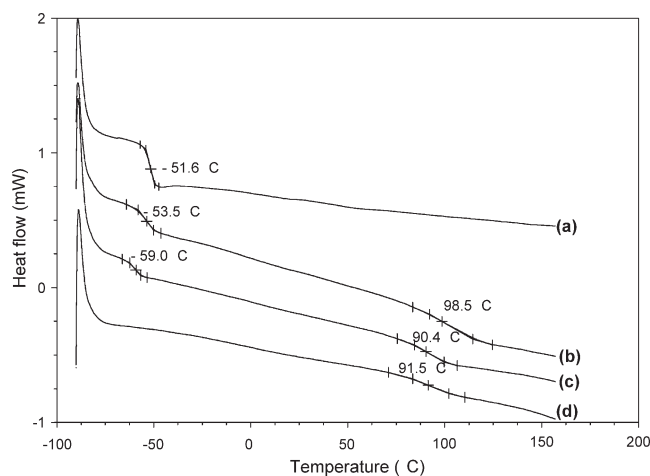

Figure 6 Thermal behavior of the NR-g-PMMAs with respect to the graft density and PMMA content: DSC curves for (a) NR1-g-PMMA9, (b) NR2-g-PMMA51, (c) NR1-g-PMMA68, and (d) NR3-g-PMMA86.

Scientific 100-W lamp placed 10 cm from the wall of the glass reactor.[25,26] After grafting, the isolated product was systematically extracted with acetone with a Soxhlet extractor to eliminate the PMMA homopolymer that possibly formed.

Thermal, morphological, and mechanical properties of NR-g-PMMA copolymer samples, free of the homopolymer, were studied as a function of the NR/PMMA composition and graft density. The purpose was not only to determine under what conditions the NR-g-PMMAs showed the characteristics of thermoplastic elastomers but also to evaluate the influence of the graft density and PMMA content on the physical and mechanical properties.

Each of the synthesized copolymers was labeled NRx-g-PMMAy, NRx referring to the DEDT-NR initially used as the macroinitiator (NR1, NR2, or NR3) and y being the PMMA content in the copolymer (wt %).

Thermal behavior of the synthesized copolymers

Typical DSC curves for various samples of NR-g-PMMAs are given in Figure 6. DSC analyses show that the thermal behavior of the copolymers varies in relation with not only the PMMA content but also the graft density (Fig. 7).

Except for copolymers with very high levels of 1,4-polyisoprene structures or conversely copolymers very rich in PMMA, all intermediate products show two T_g values, one corresponding to the glass transition assigned to 1,4-polyisoprene structures in NR domains (T_{g1}) and the other corresponding to the PMMA grafts [T_{g2}; Fig. 6(b,c)]. This result means that, under these conditions, there is phase separation, and the product shows the characteristics of thermoplastic elastomers when the PMMA content is
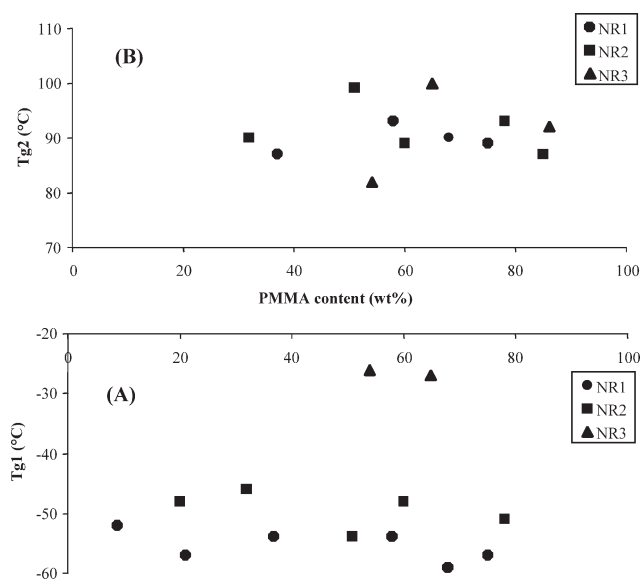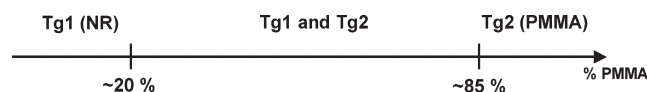
Figure 7 Progression of the T_g values with respect to the graft density and PMMA content in NRx-g-PMMAy: (A) T_{g1} and (B) T_{g2}.

about 20% (Scheme 2). If the content in PMMA is low, that is, lower than approximately 20%, only one thermal answer is observed, which corresponds to the 1,4-polyisoprene structures of NR [Fig. 6(a)]. PMMA is then dispersed within NR, and the product is macroscopically homogeneous. Conversely, when the PMMA content is very high, that is, higher than approximately 85%, only T_{g2} for PMMA is noted [Fig. 6(d)], and this shows that, in this case, NR is dispersed within the PMMA matrix.

As for the T_g values, T_{g1} and T_{g2} remain hardly affected by the PMMA content in the copolymer when the graft density is the same (Fig. 7). However, with equal PMMA contents, T_{g1} shifts toward the higher temperature side with increasing graft density according to the following order: −27 (NR3), 49 (NR2), and 56°C (NR1) [Fig. 7(A)]. In comparison with what is observed for ENRs, this result appears logical and can be explained by rigidification of the elastomer backbone with an increase in the functionalization degree. At the same time, the T_{g2} values vary irregularly between 90 and 100°C, but such variations cannot be assigned to a possible influence of the graft density [Fig. 7(B)].

Thermal stability of the synthesized copolymers

Figure 8 shows TGA curves for NR, 20% ENR (ENR20), NR2, and NR2-g-PMMA32. Despite a deg-

radation onset delayed with respect to the other rubbers, NR is less stable.

The thermal degradation of NR-g-PMMAs always occurs in two steps, whatever the content of grafted PMMA is (Fig. 8 and Table I). The obtained degradation curves show that the materials are stable up to 165°C. Beyond that, a first degradation step takes place with a low weight loss of about 3.5–7.5%, and then a second step occurs between 320 and 475°C.

It is difficult to explain all the mechanisms that contribute to the first step of degradation of NR-g-PMMA compounds. However, by comparing the shapes of TGA curves for NR, ENR20, and NR2-g-PMMA32, we find that it is likely that this first degradation step corresponds to decomposition of residual oxirane rings and DEDT functions (Fig. 8). Indeed, in contrast to NR degradation, which takes place in only one step, that is, between 320 and 460°C, with a maximum degradation rate at 380°C, ENR20 begins to degrade at a lower temperature, and two steps are observed: the first one takes place between 160 and 320°C, with a low weight loss of about 3.5%, and the second takes place between 320 and 475°C, with T_{max} at 397°C; it is therefore higher than T_{max} of NR. Consequently, in the case of ENR20, the epoxidized polyisoprene units break up at first by the generation of water molecules. As for DEDT-NR, it also degrades in two steps: the first step occurs between 160 and 320°C, with a weight loss of about 4.5%; therefore, it is a little higher than in the case of ENR20 (3.5%). This indicates that the first degradation step likely corresponds to the decomposition of the residual oxirane rings and DEDT functions.

In addition, it is worth noting that, in comparison with the other rubbers tested, DEDT-NR is the most stable; its second degradation step occurs between 320 and 475°C with T_{max} at 401°C, that is, higher
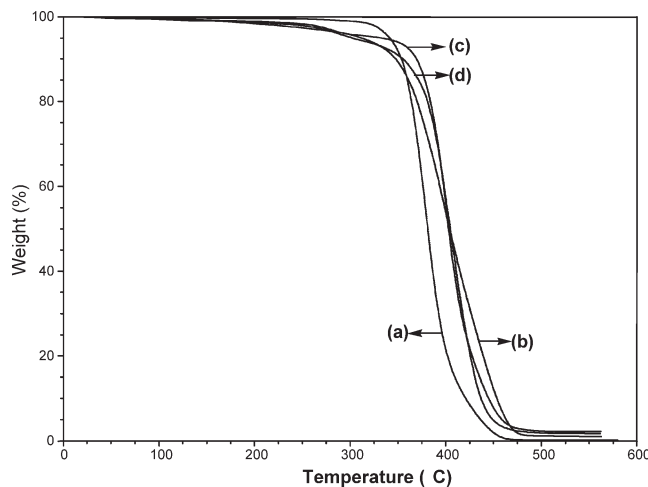

Figure 8 TGA curves for (a) NR, (b) ENR20, (c) NR2, and (d) NR2-g-PMMA32.

Tg1 (NR)   Tg1 and Tg2   Tg2 (PMMA)

~20 %   ~85 %   % PMMA

Scheme 2

TABLE I
Characteristics of the Degradation of NR-*g*-PMMAs with Respect to the Graft Density and
PMMA Content in the Graft Copolymer

Sample	Content of grafted PMMA (%)	Thermal degradation steps			
		First step		Second step	
		T_{max} (°C)	Loss of weight (%)	T_{max} (°C)	Loss of weight (%)
NR	—	—	—	380	99.6
ENR20	—	270	3.5	397	95.2
NR2	—	281	4.5	401	93.0
NR1-*g*-PMMA9	9	263	5.3	397	93.4
NR1-*g*-PMMA20	20	267	3.7	387	93.0
NR1-*g*-PMMA37	37	298	4.6	401	92.5
NR1-*g*-PMMA58	58	294	4.5	405	92.3
NR1-*g*-PMMA68	68	193	5.5	406	92.4
NR1-*g*-PMMA75	75	174	5.6	391	91.9
NR2-*g*-PMMA20	20	290	5.1	406	93.1
NR2-*g*-PMMA32	32	288	5.9	405	92.2
NR2-*g*-PMMA51	51	292	5.4	408	93.3
NR2-*g*-PMMA60	60	293	3.5	404	94.5
NR2-*g*-PMMA78	78	170	6.0	410	92.1
NR2-*g*-PMMA85	85	168	6.8	403	91.5
NR3-*g*-PMMA54	54	276	7.3	406	91.4
NR3-*g*-PMMA65	65	289	7.4	414	91.8
NR3-*g*-PMMA86	86	177	6.8	402	92.7
PMMA	—	320	19.4	388	80.2

than the ones noted for NR ($T_{max} = 380°C$) and ENR20 ($T_{max} = 397°C$). This clearly demonstrates that the stability of the *cis*-1,4-polyisoprene units of NR is reinforced after the decomposition of DEDT functions and the residual oxirane rings.

The results summarized in Table I show that, whatever the PMMA content is, the NR-*g*-PMMAs are always thermally more stable than NR: T_{max} values can be observed between 400 and 410°C, that is, at temperatures higher than that noted for NR ($T_{max} = 380°C$). It can also be seen that the degradation is not affected by the PMMA content in the copolymer.

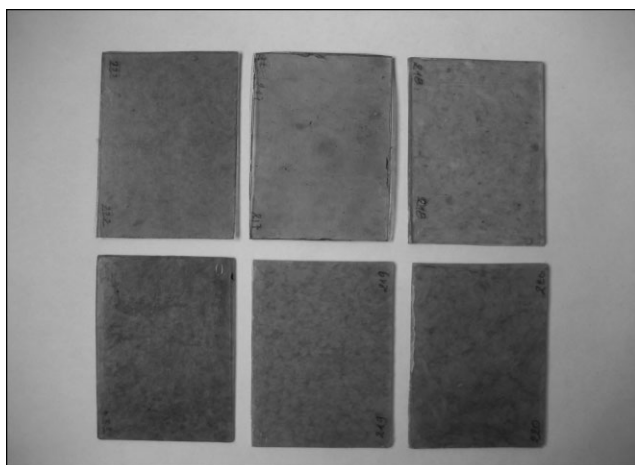## Tensile and hardness properties of the synthesized copolymers

The mechanical properties of PMMA-grafted NR samples were assessed through tensile and hardness testing. Six samples, synthesized by MMA photo-polymerization initiated by NR1 and NR2 macro-iniferters, were studied: NR1-*g*-PMMA21, NR2-*g*-PMMA23, NR1-*g*-PMMA62, NR2-*g*-PMMA64, NR1-*g*-PMMA74, and NR2-*g*-PMMA75. These different PMMA-grafted NR samples were compression-molded into small plaques (Fig. 9) from which test pieces were die-cut, as described in Figure 3.

Figure 10 shows the tensile curves recorded with 20% PMMA-grafted NR samples, which were prepared with NR1 (NR1-*g*-PMMA21) or NR2 (NR2-*g*-PMMA23). The slightly grafted samples exhibited essentially the behavior of an elastomer with relatively high elongation at break (22% for NR2-*g*-PMMA23 and 43% for NR1-*g*-PMMA21) and
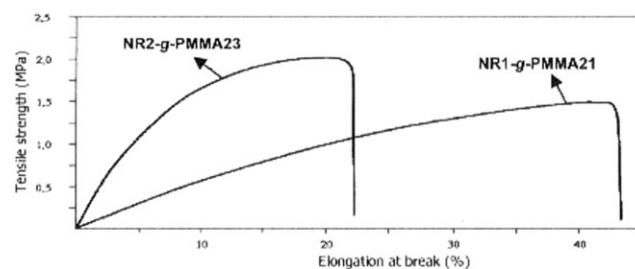
Figure 9 Photographs of plates prepared from the NR-*g*-PMMAs.

Figure 10 Stress–strain curves of NR1-*g*-PMMA21 and NR2-*g*-PMMA23 as a function of the graft density.

**Mechanical Properties of NR-*g*-PMMAs with Respect to the Graft Density and
PMMA Content in the Graft Copolymer**

Sample	Content of grafted PMMA (%)	Tensile strength (MPa)	Modulus at 10% deformation (MPa)	Elongation at break (%)	Hardness (Shore D)
NR1-*g*-PMMA21	21	1.5	1.2	43	34
NR2-*g*-PMMA23	23	2.0	1.9	22	43
NR1-*g*-PMMA62	62	11.8	9.0	6.5	75
NR2-*g*-PMMA64	64	20.0	16.7	4.0	79
NR1-*g*-PMMA74	74	16.4	14.6	3	81
NR2-*g*-PMMA75	75	25.3	—	2	82

relatively low tensile strength (in the 1.5–2 MPa range). Moreover, the elongation at break of NR1-*g*-PMMA21 was significantly higher than that of NR2-*g*-PMMA23 with, in the mean time, lower strength. This demonstrates the importance of the structural parameter because both samples had nearly identical PMMA contents but differed in the length of the grafted branches and their density in the copolymer. This result shows that interactions between chains are stronger when the grafts are numerous but short and that sliding of *cis*-1,4-polyisoprene chains over one another is therefore more difficult. Indeed, chain mobility and hence sliding in NR-*g*-PMMA are hindered when the level of associations between PMMA branches is higher (and therefore physical crosslinking is also more important).

In contrast, PMMA-grafted NR samples with high levels of PMMA exhibited weak elongation at break (in the 2–6.6% range) and high tensile strength (12–25 MPa; Table II); this behavior is typical of thermoplastic materials.

In terms of hardness (Table II), an increase with the level of grafted PMMA has been observed, as expected. However, at a constant level of PMMA, PMMA-grafted NR samples prepared by photopolymerization initiated by NR2 were harder, but the difference decreased as the grafted PMMA level increased.
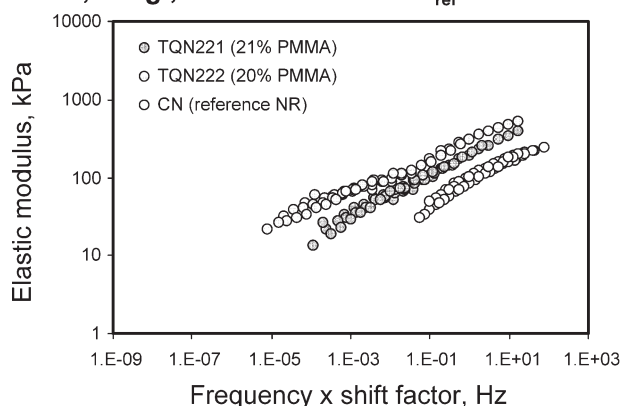
Viscoelastic properties of the synthesized copolymers

G' and G'' master curves at 120°C for all the investigated samples are given in Figures 11–13, and the corresponding values of parameters C_1 and C_2 are given in Table III. As can be seen, the mechanical properties of the grafted NR vary proportionally with the grafted content, with differences at an equal PMMA level that are likely due to structural differences in the grafted material. With around 20% grafted PMMA, the material remains essentially rubbery, while already differing from pure NR. The 64 and 75% grafted PMMA materials are typical thermoplastics.

Morphology of the synthesized copolymers

TEM was used to investigate the morphology of PMMA-grafted NRs with respect to the PMMA content in the copolymer. Figure 14 shows the morphology of two samples with very different PMMA contents, NR2-*g*-PMMA23 and NR2-*g*-PMMA75, but both showed two T_g values. They were analyzed as very thin films and were previously stained with OsO_4 (see the Experimental section) to distinguish

RPA ;1 deg ; G' mastercurve at T_{ref} = 120°C

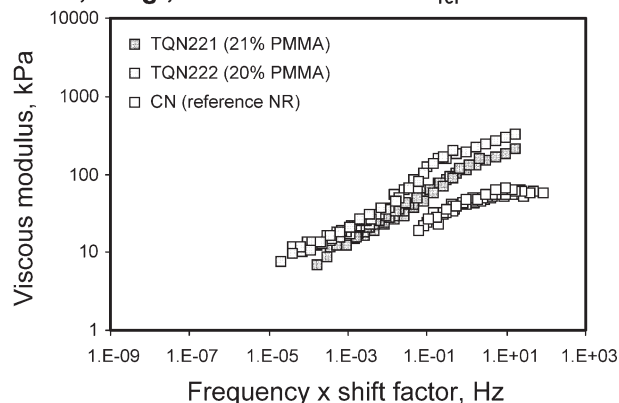**RPA ;1 deg ; G" mastercurve at T_{ref} = 120°C**

Figure 11 G' and G'' master curves at 120°C for about 20% NR-*g*-PMMA samples versus pure NR (see Table III for the C_1 and C_2 fitting parameters of the WLF-type equation).
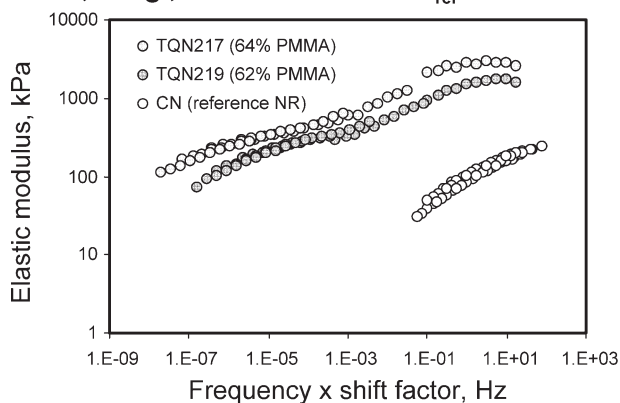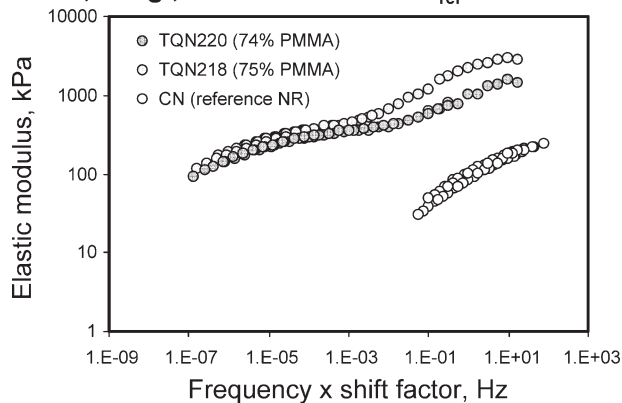
Figure 12 G' and G'' master curves at 120°C for about 63% NR-g-PMMA samples versus pure NR (see Table III for the C_1 and C_2 fitting parameters of the WLF-type equation).
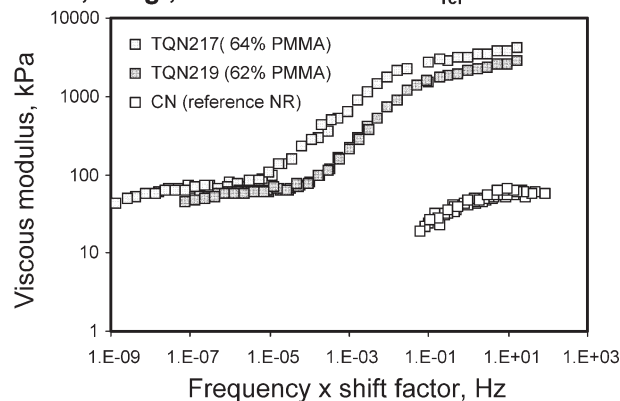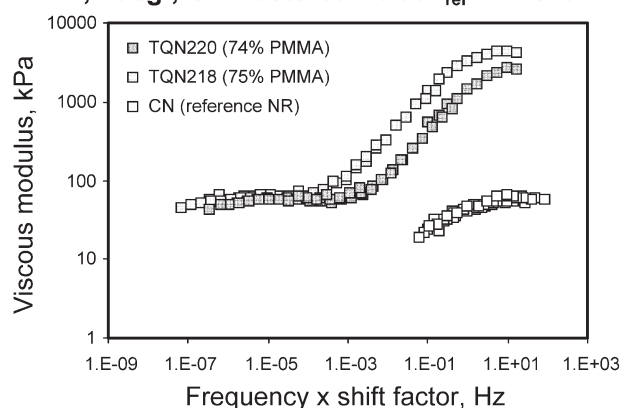

Figure 13 G' and G'' master curves at 120°C for about 75% NR-g-PMMA samples versus pure NR (see Table III for the C_1 and C_2 fitting parameters of the WLF-type equation).

the phase arrangement in the copolymer: darkness for the NR domains and clearness for the PMMA domains. When the content of PMMA is low [the case of NR2-g-PMMA23; Fig. 14(A)], PMMA grafts are gathered in the form of nodules (white domains) dispersed within the rubber matrix (dark domains). Under these conditions, in terms of morphology, NR-g-PMMAs appear as networks made up of entangled *cis*-1,4-polyisoprene chains bound between themselves by PMMA nodules (Fig. 15). On the other hand, when the content of PMMA is high [the case of NR2-g-PMMA75; Fig. 14(B)], the rubber is dispersed as nodules (dark zones) within a continuous PMMA matrix.

CONCLUSIONS

Well-defined NR-g-PMMAs were prepared to study the relationships between the structure and the properties. Syntheses were achieved by the photopolymerization of MMA initiated by DEDT groups created beforehand in side positions on the NR chains.[24–26] With this procedure, good control of the graft density and the PMMA content was obtained.

Thermal, morphological, and mechanical properties of NR-g-PMMA copolymers were studied as a function of the NR/PMMA composition and graft density.

Analyses by DSC showed that NR-g-PMMA samples very rich in 1,4-polyisoprene (>80%) or

TABLE III
Fitting Parameters C_1 and C_2 for WLF at 120°C

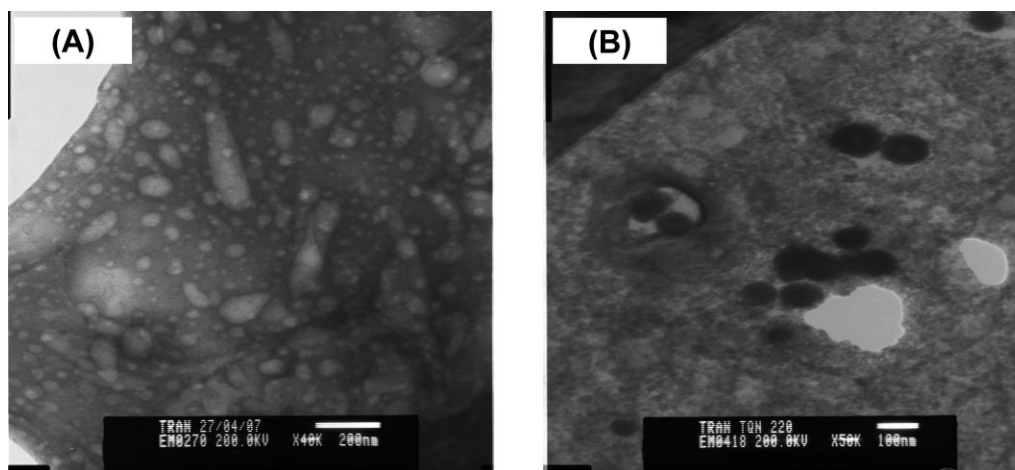| Sample		C_1	C_2	r^2
NR	G'	1.42	189.80	0.962
	G''	0.57	92.76	0.999
NR1-g-PMMA21	G'	6.77	127.75	0.996
	G''	5.55	99.73	0.980
NR2-g-PMMA23	G'	7.39	80.52	0.990
	G''	5.47	48.61	0.995
NR1-g-PMMA62	G'	9.32	60.70	0.997
	G''	10.71	74.32	0.996
NR2-g-PMMA64	G'	10.48	56.22	0.994
	G''	14.43	83.63	0.998
NR1-g-PMMA74	G'	14.32	143.78	0.999
	G''	13.04	139.02	0.953
NR2-g-PMMA75	G'	9.72	67.06	0.994
	G''	12.54	102.94	0.969

Figure 14 TEM micrographs of NR-g-PMMAs with respect to their PMMA content (OsO$_4$ stain): (A) NR2-g-PMMA23 and (B) NR2-g-PMMA75.

conversely very poor (<15%) exhibited two DSC responses, one corresponding to the glass transition of the *cis*-1,4-polyisoprene structures (T_{g1}) and the other corresponding to the glass transition of PMMA grafts (T_{g2}). This result is typical of a heterogeneous material made of two phases, one rubbery and one thermoplastic; in other words, it corresponds to a thermoplastic elastomer when the rubbery part is greater and to a softened thermoplastic when it is lesser. When the thermoplastic phase content is lower than 15%, only the T_g of the *cis*-1,4-polyisoprene structures (T_{g1}) can be observed; conversely, only the glass transition of the thermoplastic component (T_{g2}) can be seen when its level is higher than 80%. T_{g1} increases with the graft content, which of course directly depends on the rate of DEDT-NR units of the macroinitiator, whereas T_{g2} remains nearly constant.

In terms of thermal stability, with respect to NR, PMMA-grafted materials degrade in two steps. The first degradation step always occurs with a low weight loss (3–8%), which corresponds to the decomposition of the residual oxirane rings and of the residual DEDT groups. The second step corresponds to the decomposition of 1,4-polyisoprene chains of NR and PMMA grafts. T_{max}, in the 390–410°C bracket for NR-g-PMMA samples, is always higher than that for raw NR (T_{max} = 380°C); this demonstrates that the addition of PMMA grafts onto the NR chains improves the thermal stability.

Tensile and hardness tests were performed to evaluate the mechanical behavior of PMMA-grafted NRs. Tensile tests have shown that through the variation of the elastomer/thermoplastic ratio, it is possible to obtain a whole range of products with tailored properties. Materials with low contents of grafted PMMA behave as elastomers with relatively high elongation at break and low tensile strength;

the reverse is obtained with high levels of grafting. These tests have particularly shown that structural aspects (the graft density and length of grafted branches) have a major influence on the elastic behavior. Moreover, as expected, the hardness directly depends on the level of grafted PMMA: the higher it is, the harder it is. However, the structure of the copolymer is important as well, particularly when the level of grafted PMMA is low.

To supplement this work on the physical characterization of the synthesized copolymers, rheological measurements and analyses by TEM were performed. The study of the viscoelastic characteristics of PMMA-grafted NRs showed that the materials remain primarily rubbery when the content of grafted PMMA is about 20%, but they are already different from those of the pure NR. On the other hand, PMMA-grafted NRs containing about 60–75% grafted PMMA are typically thermoplastics. TEM analyses have shown that the morphology of PMMA-grafted NRs showing two T_g values in DSC strongly depends on the content of grafted PMMA. When this content is low, the copolymers adopt the morphology of thermoplastic elastomers and appear as networks made up of entangled *cis*-1,4-
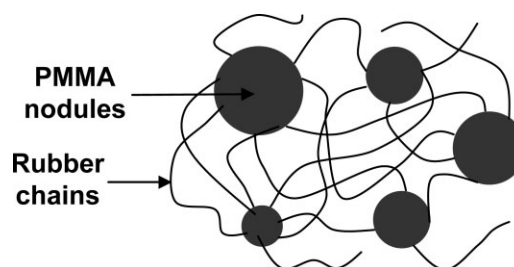

Figure 15 Diagrammatic representation of the morphology adopted by the NR-g-PMMAs when the PMMA content was low.

polyisoprene chains bound between themselves by PMMA nodules. PMMA nodules are dispersed within the rubber matrix. When the PMMA content is high, rubber nodules are dispersed in the PMMA matrix.

References

1. Brosse, J. C.; Campistron, I.; Derouet, D.; El Hamdaoui, A.; Houdayer, S.; Reyx, D.; Ritoit-Gillier, S. J Appl Polym Sci 2000, 78, 1461.
2. Derouet, D.; Radhakrishnan, N.; Brosse, J. C.; Boccaccio, G. J Appl Polym Sci 1994, 52, 1309.
3. Gelling, I. R. Rubber Chem Technol 1985, 58, 86.
4. Perera, M. C. S. J Appl Polym Sci 1987, 34, 2591.
5. Perera, M. C. S.; Elix, J. A.; Bradbury, J. H. J Polym Sci Part A: Polym Chem 1988, 26, 637.
6. Roy, S.; Gupta, B. R.; Maiti, B. R. J Elast Plast 1990, 22, 280.
7. Bradbury, J. H.; Perera, M. C. S. J Appl Polym Sci 1985, 30, 3347.
8. Nakason, C.; Kaesaman, A.; Supasanthitikul, P. Polym Test 2004, 23, 35.
9. Nakason, C.; Saiwaree, S.; Tatun, S.; Kaesaman, A. Polym Test 2006, 25, 656.
10. Derouet, D.; Phinyocheep, P.; Brosse, J. C.; Boccaccio, G. Eur Polym J 1990, 26, 1301.
11. Arayapranee, W.; Prasassarakich, P.; Rempel, G. L. J Appl Polym Sci 2003, 89, 63.
12. Thiraphattaraphun, L.; Kiatkamjornwong, S.; Prasassarakich, P.; Damronglerd, S. J Appl Polym Sci 2001, 81, 428.
13. Prasassarakich, P.; Sintoorahat, P.; Wongwisetsirikul, N. J Chem Eng Jpn 2001, 34, 249.
14. Chuayjuljit, S.; Moolsin, S.; Potiyaraj, P. J Appl Polym J 2004, 95, 826.
15. Handbook of Thermoplastic Elastomers; Walker, B. M.; Ed.; Van Nostrand Reinhold: New York, 1979.
16. West, J. C.; Cooper, S. L. In Science and Technology of Rubber; Eirich, F. R., Ed.; Academic: New York, 1978; Chapter 13.
17. Mullins, L. Rubber Dev 1978, 31, 92.
18. Enyiegbulam, M. E.; Aloka, I. U. J Appl Polym Sci 1992, 44, 1841.
19. Saelao, J.; Phinyocheep, P. J Appl Polym Sci 2005, 95, 28.
20. Monteiro, M. J.; Subramaniam, N.; Taylor, J. R.; Pham, B. T.; Tonge, M. P.; Gilbert, R. G. Polymer 2001, 42, 2403.
21. Lehrle, R. S.; Willis, S. L. Polymer 1997, 38, 5937.
22. Arayapranee, W.; Prasassarakich, P.; Rempel, G. L. J Appl Polym Sci 2002, 83, 2993.
23. Arayapranee, W.; Rempel, G. L. J Appl Polym Sci 2004, 93, 455.
24. Derouet, D.; Tran, Q. N.; Ha, T. H. Eur Polym J 2007, 43, 1806.
25. Derouet, D.; Tran, Q. N.; Ha, T. H. Eur Polym J, to appear.
26. Tran, Q. N. Ph.D. Thesis, Université du Maine, 2007.
27. Otsu, T.; Yoshida, M. Makromol Chem Rapid Commun 1982, 3, 127.
28. Otsu, T.; Yoshida, M.; Tazaki, T. Makromol Chem Rapid Commun 1982, 3, 133.
29. Otsu, T.; Matsunaga, T.; Doi, T.; Matsumoto, A. Eur Polym J 1995, 31, 67.
30. Otsu, T.; Yamashita, K.; Tsuda, K. Macromolecules 1986, 19, 287.
31. Endo, K.; Murata, K.; Otsu, T. Macromolecules 1992, 25, 5554.
32. Doi, T.; Matsumoto, A.; Otsu, T. J Polym Sci Part A: Polym Chem 1994, 32, 2911.
33. Derouet, D.; Mulder-Houdayer, S.; Brosse, J. C. J Rubber Res 2006, 9, 1.